


## Enhancing Radiator Cooling with CuO Nanofluid Microchannels

Shalom Akhai<sup>1</sup> , Amandeep Singh Wadhwa<sup>2\*</sup> 

<sup>1</sup>Department of Mechanical Engineering Maharishi Markandeshwar Engineering College Maharishi Markandeshwar (Deemed to be University)  
Mullana-Ambala, Haryana – 133207 India

<sup>2</sup>UIET, Panjab University, Chandigarh-160014, India

### Abstract

The study explores in employing copper oxide (CuO) nanofluid as a cooling medium in the vehicle radiators. To simulate the heat transfer process, the microchannel is constructed using elec-tron discharge machining (EDM) and a computational fluid dynamics (CFD) modeling is em-ployed. UV-visible spectroscopy, scanning electron microscopy (SEM), and dynamic light scat-tering (DLS) are used to characterize the CuO nanofluid. CuO nanofluid surpasses water in the heat transfer capabilities, with a 40% improvement in thermal conductivity. The average size of CuO nanoparticles was determined via DLS to be 485.1 nm. The heat transfer coefficient of CuO nanofluid is 5366 W/m<sup>2</sup>K, which is 116% larger than that of water. The increased heat transfer capabilities of CuO nanofluid microchannel flow indicate to its potential as a viable replacement for conventional radiators in the automotive applications. Lower engine temperatures, increased fuel efficiency, and longer engine lifespan may result from improved cooling performance. Due of the small size of microchannels, more efficient and space-saving radiators for automobiles are conceivable. More research is needed to improve the microchannel design as well as to realize the practical benefits of CuO nanofluids in car cooling systems.

**Keywords:** CFD; COMSOL; Electron discharge machining; Micro-channel; Nano fluid

### Research Article

#### History

Received 03.12.2023  
Revised 12.01.2024  
Accepted 11.02.2024

#### Contact

\* Corresponding author  
Amandeep Singh Wadhwa  
[aman\\_wadhwa77@rediffmail.com](mailto:aman_wadhwa77@rediffmail.com)  
Address: Mechanical Department, UIET, Panjab University, Chandigarh

**To cite this paper:** Akhai, S., Washwa, A.S. Enhancing Radiator Cooling with CuO Nanofluid Microchannels. International Journal of Automotive Science and Technology. 2024; 8 (2): 201-211. <https://doi.org/10.30939/ijastech.1399702>

### 1. Introduction

Computers, electronics, and communication have evolved considerably in recent decades. Power consumption and data storage in small chips have risen with these devices, making thermal management harder [1,2]. These air-coolers are at capacity. Applications exceeding 100W/cm<sup>2</sup> need advanced cooling [3]. Today, liquid cooling solves these challenges. These fluids' thermal conductivity makes energy-efficient heat transfer devices [4-6]. Despite substantial heat transfer improvement research, heat transfer fluids have weak thermal conductivity, limiting cooling [7, 8]. At normal temperature, solid metals have far greater thermal conductivities than fluids [9,10]. Heat flows better via metallic liquids. Thus, suspended solid metallic particle fluids should have better thermal conductivity than heat transfer fluids. Advanced applications need heat dissipation beyond water. Most solids transmit heat better than conventional heat transfer fluids [11,12]. Thus, liquid-fluid microchannel heat sinks efficiently manage electrical and optical device temperatures. Micro channels are smaller, have less coolant inventory, and have a bigger heat transfer surface, making them useful in automotive, aerospace, refrigeration, air conditioning, gas turbine blade

cooling, and processing [13-16]. They have low channel pressure drop and strong convective heat transfer coefficient [17,18]. Although pressure drop was high, Tuckerman and Pease [19] used direct water circulation in rectangular micro channels to reduce heat flux up to 790 W/cm<sup>2</sup> utilizing silicon microchannels for electronics cooling in 1981. Peng et al. [20] carried out studies on water flow fluctuations in rectangular micro channels. Kawano et al. [21] explored water-coolant pressure drop and heat transfer statistically and experimentally. Simulated pressure loss was lower than Reynolds number testing above 300. Channel thermal resistance raised to 0.1K/W.cm<sup>2</sup> with 100W/cm<sup>2</sup> heat flow. Yin et al. studied pressure loss in one-phase microchannel heat exchangers with parallel circuits and intricate headers [22]. These measurements revealed manufacturing issues. Moody chart friction factors were determined. Kim [23] suggested 3-D modeling of microchannel heat sink thermal resistance utilizing a fin model, porous medium model and optimization. In a microchannel heat sink, Min et al. [24] simulated the influence of tip clearance. Xu et al. [25] split the flow domain into longitudinal and transverse microchannel zones to form a microchannel sink. Lee and Garimella [26] studied heat transmission in copper micro channels of 194-534µm

diameters and 300-3500 Reynolds numbers. Wang et al. [27] developed a computer model to evaluate nanofluid cooling micro-channel thermal and hydraulic performance. With fixed pumping power, pressure drop, and volume flow rate, channel number and aspect ratio were optimized. A silicon micro-nano pillar multilayer water-cooled heat sink was created by Dixit et al. The researchers found that silicon pillars increased heat dissipation. In ethylene glycol, de-ionized water, and oil, Choi and Eastman [29] distributed nanocrystalline particles to enhance heat transfer. Reiyu Chein and Janghwa Chen studied microchannel heat sink fluid flow and heat transfer using numerical FVM [30]. P. Gunnasegaran et al. [31] calculated water flow pressure drop and friction factor in rectangular, trapezoidal, and triangular microchannel heat sinks for 100–1000 Reynolds numbers using finite volume technique. Wang et al. [32] provides an overview of nanofluid heat transfer characteristics, as well as enhancements and challenges in using nanofluids for heat transfer applications in microchannels. Timofeeva et al. [33] investigate the effect of particle shape on the thermophysical properties of alumina nanofluids, contributing to a better understanding of particle morphology's role in heat transfer enhancement. The investigation of the viscosity data for  $\text{Al}_2\text{O}_3$ -water nanofluid and the enhancement of heat transfer based on nanofluid viscosity behavior was conducted by Nguyen et al. [34]. The temperature dependent thermal conductivity and viscosity of  $\text{TiO}_2$ -water nanofluids are investigated by Duangthongsuk et al. [35] which is critical for understanding their heat transfer behavior at different temperatures. Putra et al. [36] explored the heat transfer trend in nanofluid microchannel flow under natural convection conditions. Ho, Wei and Li [37] studied the performance of microchannel heat sinks with  $\text{Al}_2\text{O}_3$ -water nanofluids, highlighting their potential for improved heat transfer over conventional coolants. Xie, Lee and Youn [38] investigated multi-walled carbon nanotube containing nanofluids and their improved thermal conductivities, contributing to a better understanding of nanofluid behavior with various nanoparticle materials. An experimental investigation of the forced convective heat transfer coefficient of nanofluids in a helically dimpled heat exchanger under turbulent flow conditions is carried out by M. Mehrali et al. [39], providing perspective for the heat exchanger design. Chon et al. [40] developed an empirical correlation relating temperature and particle size to the thermal conductivity enhancement of  $\text{Al}_2\text{O}_3$  nanofluids, allowing for more accurate predictions of nanofluid thermal conductivities. Ghadimi et al. [41] examined the properties of nanofluid stability and characterization methods in stationary conditions, which are critical for understanding nanofluid behavior in heat transfer applications.

### 1.1. Limitations of the previous study

Research on microchannel heat flow with and without nanofluids has improved heat transfer techniques. However, these studies have struggled to achieve true adiabatic conditions in experimental setups, address nanofluid stability, standardize experimental protocols, explore microchannel design param-

eters and consider nanofluid degradation. Since actual experiments generally include friction losses, pressure drops, and heat transmission to the surroundings, achieving real adiabatic conditions is difficult. The detailed knowledge of nanofluid concentration's nonlinear impact on heat transfer performance requires a greater emphasis on individual concentrations. Standardized procedures across research would improve repeatability and dependability. Further scaling the microchannel heat transfer to the industrial level at low cost while maintaining efficiency remains a challenge. The transient behavior of microchannel heat flow and its dynamic response needs further investigation for applications requiring rapid response.

### 1.2. Research gaps

Microchannel heat flow using nanofluids has advanced, yet there are certain research gaps. A thorough knowledge of the effect of nanofluid concentration on heat transfer performance is needed. While there are numerous microchannel designs, research is ongoing to determine the most efficient and effective geometries for specific applications. This entails experimenting with various shapes, aspect ratios and surface modifications to improve heat transfer. Researchers are investigating methods such as using nanofluids, additives or surface coatings to improve convective heat transfer coefficients, as well as investigating pulsating flows for improved performance. Understanding heat transfer phenomena at the nanoscale within microchannels is an area that is still largely unexplored. Investigating the effects of molecular dynamics, phonon transport and material interactions at this scale could greatly improve the understanding and efficiency in microscale heat transfer. Microchannel fabrication and manufacturing techniques require improvement. Techniques for creating complex microchannel structures that are cost-effective, scalable and precise are critical for practical implementation. The research to investigate heat transfer in microchannels under phase change conditions, especially for applications such as thermal management and refrigeration systems is still in nascent stage.

### 1.3. Objective of the experimentation

The aim of the current study is to prepare the nanofluid and conduct morphological analysis of the nanofluid to determine the size and dispersion of nano particles in the base fluid. CFD analysis is performed using COMSOL Multiphysics software to investigate the flow of nanofluid through rectangular microchannel. The theoretical results (COMSOL software) of the heat transfer coefficient for the flow of water and  $\text{CuO}$  nanofluid through rectangular microchannel are compared with the experimental results. The effect of velocity, Reynolds number and Nusselt number on heat transfer coefficient of water and  $\text{CuO}$  nanofluid and the dependence of Nusselt number on Reynolds number for water and  $\text{CuO}$  nanofluid is investigated. The research developed the microchannel heat flow system with high heat dissipation rate which can be employed effectively in the automobile radiator cooling resulting in cost effectiveness and eco- friendly environment.

## 2. Design and fabrication of Microchannel

The microchannel in the shape of a rectangle was developed on Solid works 2014 as shown in Figure 1. Measurements such as length, height, breadth, hydraulic diameter, height of substrate, and width of substrate are among the different geometrical features that are associated with rectangular microchannels (Table 1). Polycarbonate was utilized for the cover plate, which worked as both a sealer and an insulator because of its dual purpose. On this cover plate, two general assemblies were machined, and they were connected to the microchannel in order to frame the test section. Both the three-dimensional rectangular shape and the manufactured model are shown in Figure 2. Copper was chosen as the material for the substrate because of its high heat conductivity of 385W/mK. Additionally, channels were formed on the substrate by the use of micro precision wire electron discharge machining. There were several phases of planning that went into the design of the microchannel heat sink. The test piece also known as foundation plate was made of aluminum 6061 alloy.

## 3. Characterization of the nano fluid

UV spectroscopy was used in order to study the characteristics of the nanofluid that was generated using CuO nanoparticles. For the purpose of morphology and particle size analysis, further SEM and DLS were used. For the purpose of recording the spectra of CuO nanofluid, UV-visible spectroscopy was used. The ultraviolet spectrum has been recorded from 200 nm to 700 nm, and the absorbance peak occurs at 237 nm in CuO nanofluid. This peak is attributed to the transition from  $\pi \rightarrow \pi^*$ , as seen in

Figure 3. It is possible to monitor the reaction process by UV-visible spectroscopy, which is made possible by the production of stable CuO dispersions. The scanning electron microscopy (SEM) technique has been used in order to investigate the surface morphology of the CuO nano particles. By placing a little quantity of liquid drop on a silicon wafer, as shown in Figure 4, and then drying the mixture for twenty-four hours in an airtight container, a very thin film of copper oxide was produced. This was done to prevent any moisture or dirt from getting into the film. After that, a scanning electron microscope (SEM) picture of a powdered thin film sample that had been dried was acquired, as shown in Figure 5. A picture obtained from a scanning electron microscope (SEM) may be used to clearly see the surface morphology, as shown in Figure 6, which demonstrates the homogeneity in the dispersion of CuO nano particles

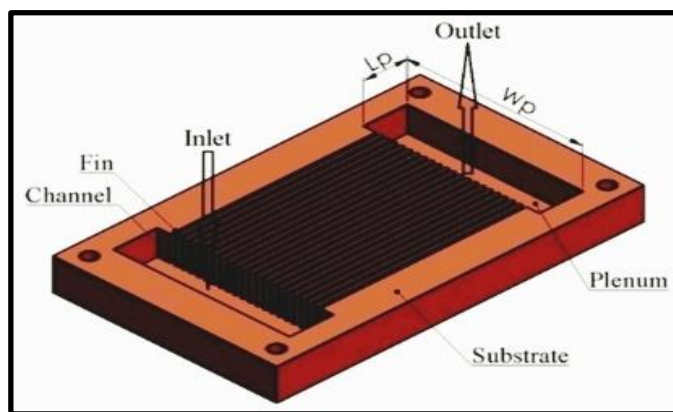


Fig.1. Rectangular Microchannel.

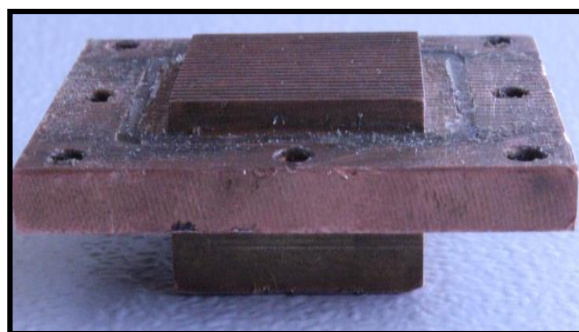


Fig.2.3D microchannel and fabricated model

Table 1. Geometric Dimensions of Rectangular Microchannel

Width of channel (mm)	Height of channel (mm)	Width of substrate (mm)	Height of substrate (mm)	Length of microchannel (mm)	Number of channels
$W_c$	$h_c$	$W_s$	$H_s$	$L$	$N$
0.5	4	37.5	10	20	21

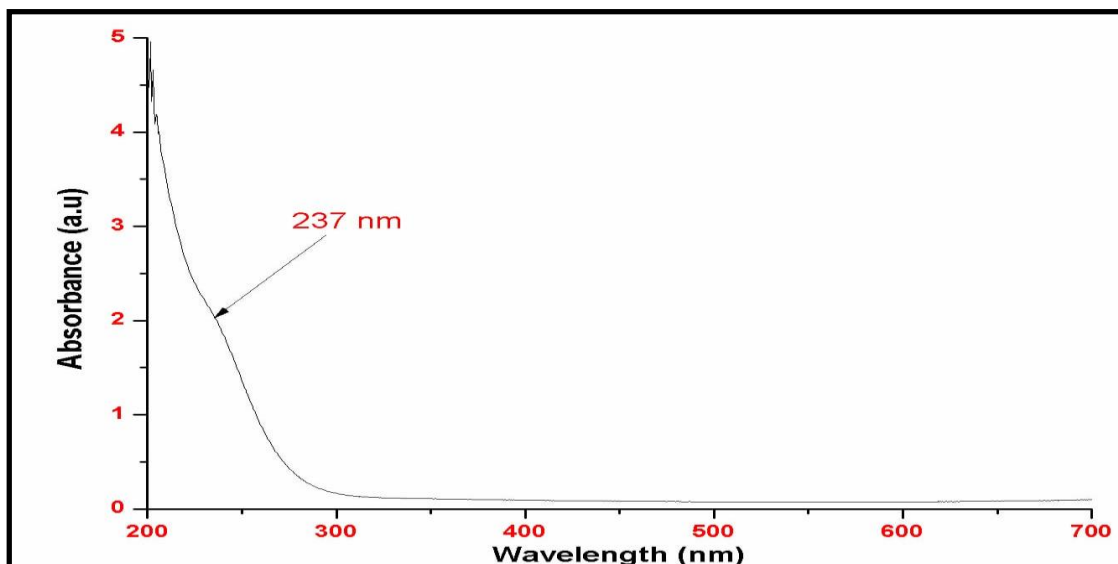


Fig.3. UV-visible absorbance spectra of CuO nanofluid



Fig. 4 CuO Sample for SEM

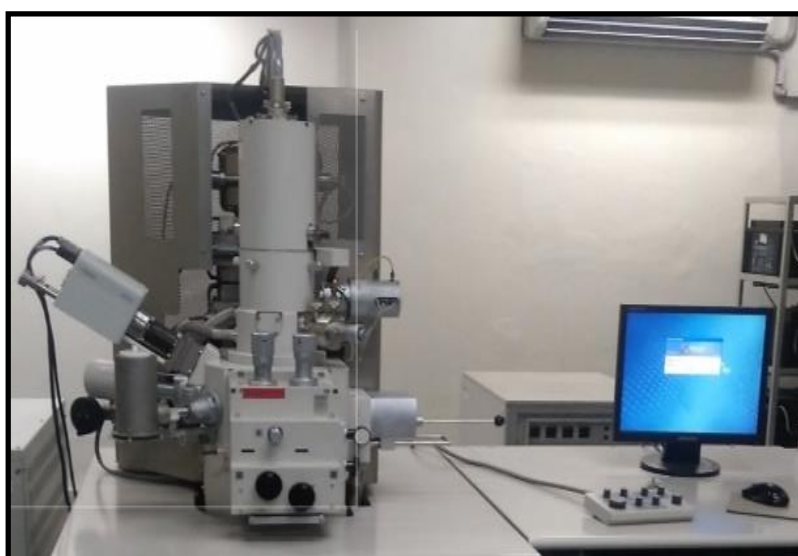


Fig. 5 SEM (KYKY-EM3200/China)



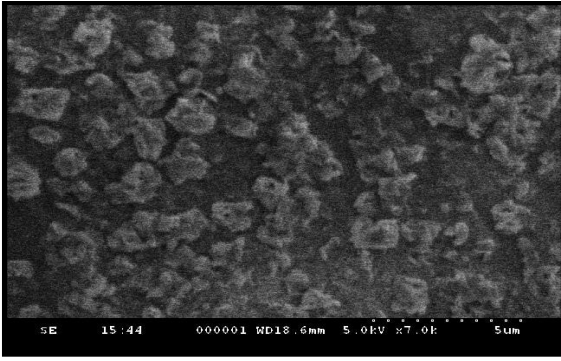


Fig. 6 SEM Image of CuO

In order to determine the average particle size distribution of copper oxide nanoparticles, the Dynamic Light Scattering technique was used. At the beginning of the nanofluid formation process, it was found that the sample of CuO nanofluid had an average particle size distribution of 485.1 nanometers. In Figure 7, the different characteristics of the system are as follows: temperature (25 degrees Celsius), measuring location (3 millimeters), count rate (7.2 kilocycles per second), duration (50 seconds), and attenuator (11).

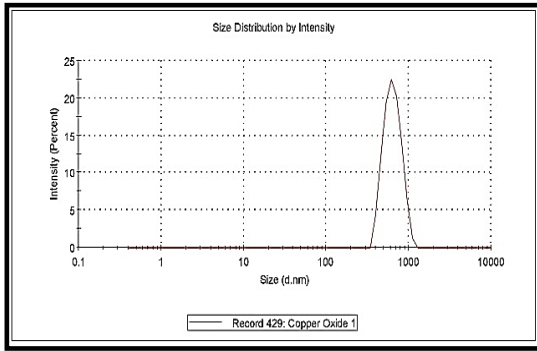


Fig. 7. CuO particle size measurement using DLS

#### 4. CFD modeling of microchannel heat sink

The formulation of a computational fluid dynamics (CFD) model to study the thermal performance of a rectangular microchannel heat sink using water and the suggested nanofluid as the working fluid has been done in this section. The COMSOL Multiphysics program was used to model and simulate a rectangular microchannel in single phase flow. The dimensions of the microchannel were identical to those of the real experimental test setup. The finite element method known as COMSOL Multiphysics is used to simulate flow in all velocity regimes, provided the boundary conditions. This is accomplished by solving numerous variants of the Navier Stokes equations. Both the design and simulation of the microchannels were accomplished with the assistance of the structural mechanics and physics component of the MEMS Tool known as COMSOL. Figure 8 illustrates the meshing of the microchannel that is rectangular in shape. Structured mesh with triangular elements was used for meshing the geometry as shown in Figure 8. 100 X100 X10 nodes were created with element size of 0.0005 in all the three dimensional coordinates. The solution based on the governing equations and discretized mesh took 1000 iterations to converge.

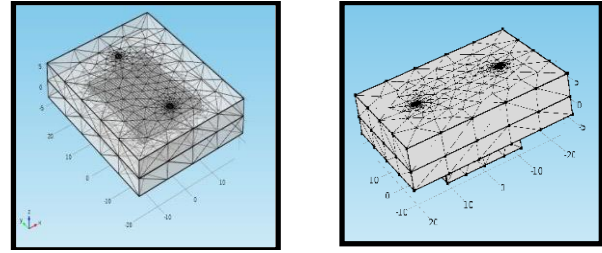


Fig. 8. Meshed microchannel design of rectangular microchannel

CFD analysis predicted heat and mass transfer, fluid flow and related phenomena by solving simultaneous set of following governing numerical equations which include continuity, momentum and energy equations for fluid and solid.

$$\nabla \cdot (\rho u) = 0 \quad (1)$$

$$(u \cdot \nabla) u = \nabla \cdot [-pI + \mu(\nabla u + (\nabla u)^T - \frac{2}{3}\mu(\nabla \cdot u)I) + F] \quad (2)$$

$$\rho C_p u \cdot \nabla T = \nabla \cdot (k \nabla T) + Q + Q_{vh} + W_p \quad (3)$$

$$\rho C_p u \cdot \nabla T = \nabla \cdot (K \nabla T) + Q \quad (4)$$

Initial value

$$u = 0, P = 0, T = 293.15K$$

Fluid walls:

Boundary condition

No Slip,  $u = 0$

Inlet:

$$u = -u_0 n = \text{Normal inflow velocity}$$

$$T = T_0 = 295.15K = \text{inlet temperature}$$

Figure 9 depicts a schematic layout of the experimental setup that was used to analyze the flow of heat through a microchannel using water and a nanofluid based on CuO at varying flow rates.

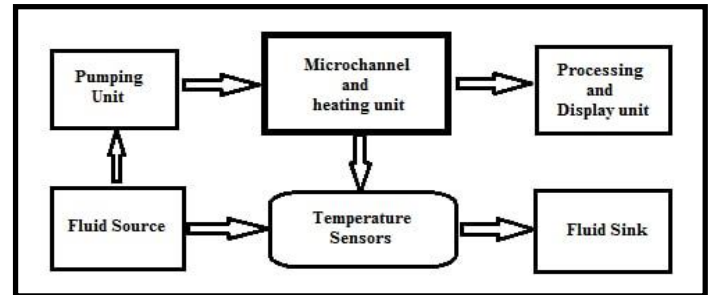


Fig. 9. Schematics of the experimental set-up

#### 5. Experimentation

In Figure 10, the experimental equipment for measuring heat flow via microchannels is shown. All of the components that make up the experimental apparatus seen in the picture are as follows: (a) Fluid Source (b) A peristaltic pump (c) The thermocouple of the K-type (d) meter of wattage (e) An exchanger for heat (f) System for the collecting of data (g) The multimeter, (h) heater for plates (i) D.A.C card. As working fluids, water and nanofluids that included nanoparticles of copper oxide suspended in a base fluid (such as water that had been diluted) were used. The accuracy of the sensors of the experimental apparatus is provided in Table 6.

$$\text{Mass flowrate} = \rho AV \quad (5)$$

where the density is denoted by  $\rho$ ,  $A$  represents the area and  $V$  represents the velocity. From 45 and 240 was the range of the Reynolds number. In order to determine the temperature of both the intake and the outflow, two thermocouples of the K-type were used. In order to determine the temperature of the substrate, a multimeter was being used. As shown in Figure 11, the KD2 Pro analyzer is used for the purpose of determining the thermal conductivity of the nano fluid. The specifications of the KD2

probe are provided in Table 5. The thermal conductivity of CuO nanofluid and water were found to be 0.842 W/mK and 0.6 W/mK respectively which is within the range provided in the literature (0.5 W/mK to 10 W/mK for CuO nanofluid depending upon size and concentration of the nanoparticles and 0.5 W/mK to 0.6 W/mK for water at room temperature depending upon the impurities in it.)

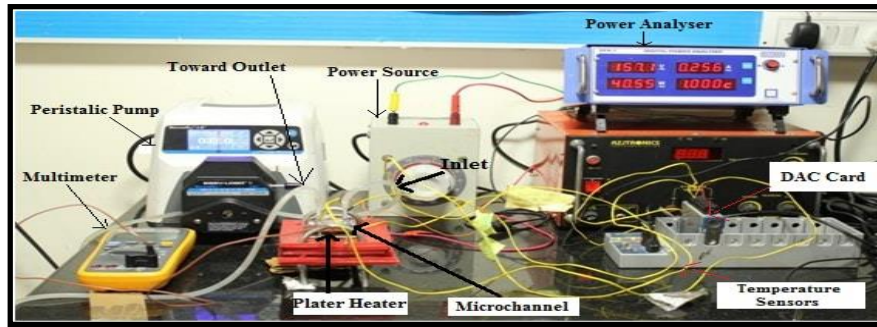


Fig. 10. Experimental apparatus

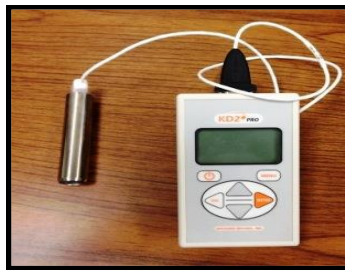


Fig. 11. KD2 probe to measure thermal conductivity

## 6. Results and Discussion

With the help of the COMSOL Multiphysics software, flow through the microchannel sink is simulated for both water and CuO nano fluid at the same flow rate (Table 2). Since it is not possible to create an adiabatic setup that is ideal, the discrepancy between the theoretical and practical findings may be attributed to the numerous losses that occur in the experimental settings which include friction loss or pressure drop and heat transfer to the surroundings.

$$h = \frac{Q}{A \Delta T_n} \quad (6)$$

where  $Q$  is the amount of heat that is applied to the substrate,  $n$  is the number of channels, which is equal to 21, and  $\Delta T$  is the difference between  $T_{wall}$  and  $T_{mean}$ . The fluctuation of the heat transfer coefficient with velocity is seen in Figure 12 for both water and nano fluids based on CuO. Table 3 presents the results of fifteen tests that were carried out by altering the heat flux and flow rate that was introduced into the system for both water and CuO nanofluid. The fluctuation in the heat transfer coefficient of water and CuO nanofluid when subjected to varying heat fluxes and flow rates while maintaining the same Reynolds number is seen in Figure 13. When both the heat flow and the Reynolds number are increased, there is a corresponding rise in the heat transfer coefficient for the flow. It was observed that the Nusselt number rises with an increase in the Reynolds number which concludes that the Nusselt number is dependent upon the Reynolds number. Nusselt number and heat transfer coefficient of both fluids are plotted against the Reynolds number at 75 W (Figure 14 and 15). As can be seen in Figure 14, the Nusselt number value for water falls somewhere in the range of 1.1 to 3.7, but the value for the suggested nanofluid falls somewhere in the range of 0.9 to 5.6. Nusselt number variation for water and nanofluid are shown in Figure 16 and Figure 17 respectively. Both of these figures demonstrate the variance of Nusselt number with respect to heat transfer coefficient.

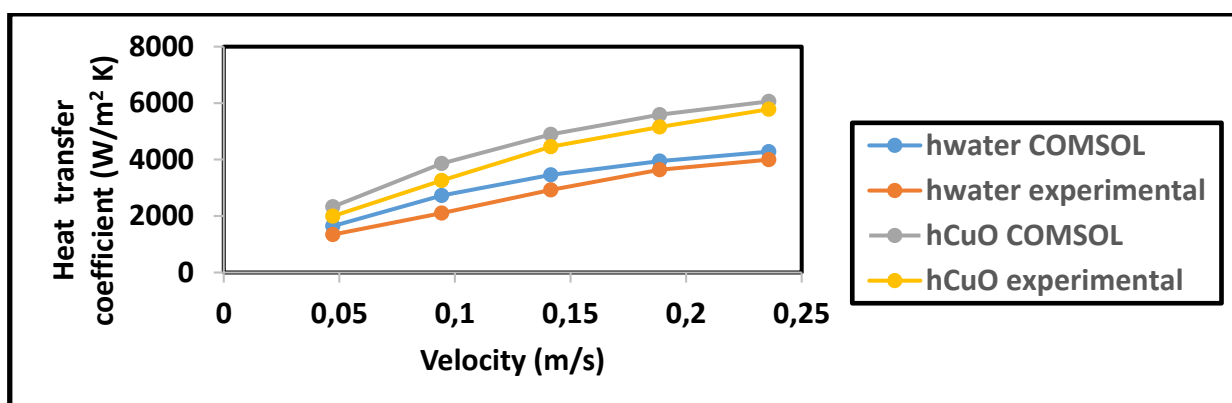


Fig. 12. Velocity vs Heat transfer coefficient for water and CuO nano fluid at 25 W

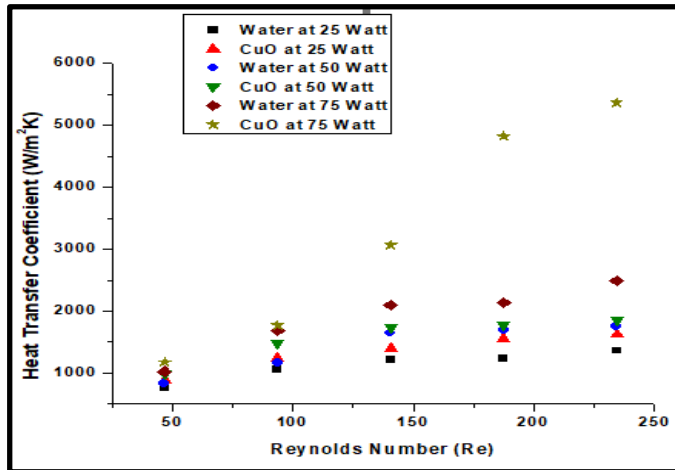


Fig. 13. Heat transfer coefficient vs Reynolds number at 20W,50W and 75W

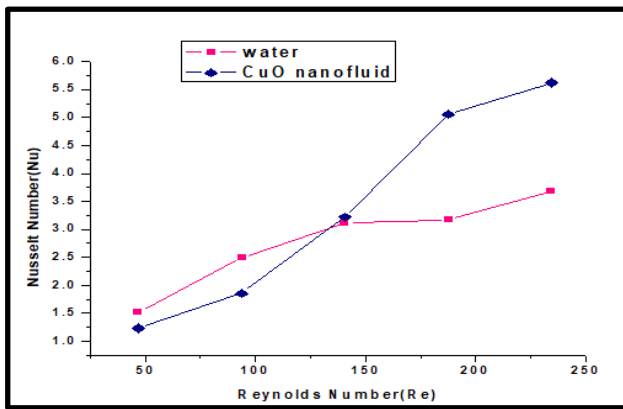


Fig. 14. Nusselt number Vs Reynolds number for water and CuO nanofluid at 75W

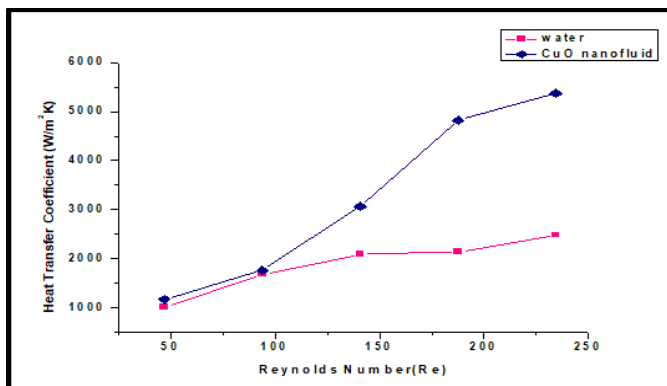


Fig. 15 Heat transfer coefficient Vs Reynold number for water and CuO nanofluid at 75 W

At a constant power input of 25 W, the heat transfer rate coefficient is influenced by the velocity of the fluid with increase in velocity the convective heat transfer rate increases assuming all other parameters remain constant. Similarly, using a CuO nanofluid, the enhanced thermal properties of the nanofluid would

lead to an increased heat transfer coefficient compared to water assuming similar conditions. The relationship between the heat transfer coefficient and the Reynolds number is crucial in understanding heat transfer in fluids, especially in forced convection scenarios at low Reynold numbers, the heat transfer is relatively lower due to less turbulence and as the Reynolds number increases and the flow transits to the turbulent regime the heat transfer coefficient tends to increase. Turbulent flow enhances mixing and increases the contact between the fluid and the surface, leading to better heat transfer. The relationship between the Nusselt number (Nu) and Reynolds number (Re) in convective heat transfer helps understand how heat is transferred from the surface to a fluid. In water, as Reynolds number increases Nu tends to increase as well. Turbulent flow promotes better mixing and increased heat transfer, resulting in a higher Nusselt number. The presence of CuO nanoparticles enhanced the thermal conductivity of the nanofluid compared to water. This alteration in thermal properties could impact the Nusselt number differently across various Reynolds numbers. Generally, nanofluids tend to exhibit higher Nusselt numbers compared to base fluids due to improved thermal properties however it is observed that Nusselt number of water is higher than the nanofluid at lower Re values.

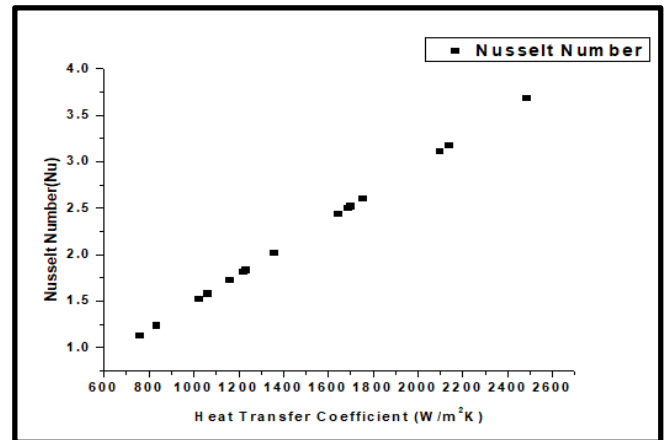


Fig.16. Nusselt Number vs heat transfer coefficient for water

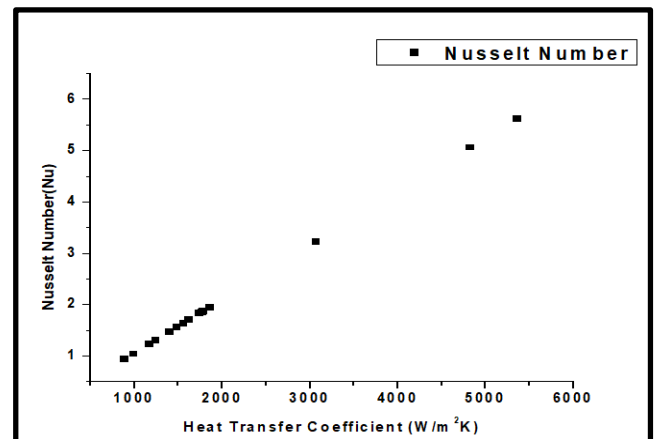


Fig.17. Nusselt Number vs heat transfer coefficient for CuO nanofluid

Table 2. Heat transfer coefficient for water and nanofluid (simulated and experimental results)

Sr. No.	Velocity (m/s)	$h_{\text{water}}(\text{W/m}^2\text{K})$ theoretical	$h_{\text{water}}(\text{W/m}^2\text{K})$ experimental	$h_{\text{CuO}}(\text{W/m}^2\text{K})$ theoretical	$h_{\text{CuO}}(\text{W/m}^2\text{K})$ experimental
1	0.0472	1642.9	1340	2327.4	1997
2	0.0943	2726.7	2104	3862.8	3257
3	0.1415	3455.5	2922	4895.4	4454
4	0.1886	3946.7	3637	5591.2	5154
5	0.2358	4280.9	3998	6064.6	5786
6	0.0472	1629.9	1426	2309	1986
7	0.0943	2710.9	2182	3840.5	3358
8	0.1415	3440.8	3120	4874.4	4457
9	0.1886	3933.8	3668	5572.9	5049
10	0.2358	4269.4	3974	6048.3	5685
11	0.0472	1568.5	1255	2222	1982
12	0.0943	2559.2	2187	3625.6	3267
13	0.1415	3230.3	3018	4576.2	4120
14	0.1886	3679	3178	5211.9	4898
15	0.2358	3976.8	3587	5633.8	5314

Table 3. Heat Transfer Coefficient at different heat flux and flow rate

Sr. No.	Flow Rate(ml/min)	Heat (W)	Re	$h_{\text{water}}(\text{W/m}^2\text{K})$	$h_{\text{CuO}}(\text{W/m}^2\text{K})$
1	20	25	47	729	860
2	40	25	94	1025	1203
3	60	25	141	1179	1357
4	80	25	188	1200	1512
5	100	25	234	1335	1592
6	20	50	47	813	982
7	40	50	94	1129	1468
8	60	50	141	1590	1724
9	80	50	188	1669	1768
10	100	50	234	1738	1858
11	20	75	47	899	1172
12	40	75	94	1374	1763
13	60	75	141	1637	3054
14	80	75	188	1666	4802
15	100	75	234	1874	5359

## 7. Conclusions and Future Scope

In the present research microchannel having rectangular dimensions was manufactured and the flow of water and CuO based nanofluid through the microchannel was analyzed experimentally and simulated using COMSOL Multiphysics software. The software is used to conduct the investigation, which is focused on the heat transfer and fluid flow analysis of water and nano fluids traveling via rectangular micro channels. CuO nanofluid microchannel flow was discovered to have a thermal conductiv-

ity that is forty percent greater than that of water-based micro-channel flow via the experimental study. When CuO nanoparticles were initially manufactured, their average size was found to be 485.1 nm using DLS technique. With the use of CuO nano fluid rectangular microchannels, it is possible to attain a high heat transmission coefficient of 5366 W/m<sup>2</sup>K, which is 116% more than the water flow through the microchannel. When the Reynolds number remains the same, the heat transfer coefficient for both the water and CuO nanofluid rises as the heat flux increases whereas at the same heat flux the Nusselt number shows



an upward trend with the Reynolds number. On the other hand, the value of the Nusselt number for CuO nanofluid is lower than water when the Reynolds number is low because of high thermal conductivity of nanofluid and it is larger than water when the Reynolds number is elevated. Because of the high thermal conductivity, the Nusselt number of CuO nanofluid is low, despite the fact that it has a high heat transfer coefficient. It is possible that the Nusselt number of CuO nanofluids might be up to 200 percent higher compared to the conventional fluid (water) at

higher heat transfer coefficient. The scope of future research is to widen the study in order to examine the wear characteristics of radiator material when nanoparticles are added to the base fluid. Extensive study can be done to increase the heat transfer coefficient by considering the appropriate suspension, the usage of microchannels with varied aspect ratios and the impact of nanofluid on double-layer microchannels can be investigated further.

Table 4. Thermophysical relations

Thermo-physical Property	Correlation
Density( $\rho$ )	$\rho_{\text{composite}} = \phi \cdot \rho_{\text{particle}} + (1 - \phi) \cdot \rho_{\text{fluid}}$ , $\phi$ is the volume fraction of nanoparticles
Specific heat(C)	$C_{\text{composite}} = \phi \cdot C_{\text{particle}} + (1 - \phi) \cdot C_{\text{fluid}}$
Dynamic Viscosity( $\mu$ )	$\mu = \mu_{\text{fluid}} \cdot (1 + 2.5 \cdot \phi \cdot \mu_{\text{particle}} + 2.5 \cdot \phi \cdot (\mu_{\text{fluid}} - \mu_{\text{particle}}) \mu_{\text{particle}} - \mu_{\text{fluid}})$

Table 5. Specifications of KD2 probe

Speed	2 minutes
Weight	148g (5 oz.)
Operating Environment	-20°C to 60°C
Power	3.0V CR2-type lithium-ion battery
Accuracy	5% Thermal Conductivity/Resistivity
Range	K (thermal conductivity): 0.02-2 Wm <sup>-1</sup> C <sup>-1</sup> R (thermal resistivity): 0.5—50 m°C/W
Needle Diameter	1.28mm
Needle Length	60 mm
Cable Length	72 cm

Table 6. Accuracy of the sensors of the experimental setup (Figure 10)

Sensor	Accuracy
Peristaltic pump	2% to 5%
K-type thermocouple	±1.5°C to ±2.2°C
Wattmeter	0.5% to 1% of full scale
Heat exchanger	Effectiveness ( $\epsilon$ ) = 0.8
Multimeter	0.5% to 1% of full scale
Plate heater	2% to 4%
DAC card	0.3% to 0.5%

## Nomenclature

h	: Heat transfer coefficient (Q/A $\Delta$ T) (W/m <sup>2</sup> K)
k	: Coefficient of thermal conductivity (QL/A $\Delta$ T) (W/mK)
Re	: Reynolds Number( $\rho V/\mu$ )
Nu	: Nusselt Number(hl/k)
$\rho$	: Density (kg/m <sup>3</sup> )
Q	: Heat flux Watt
V	: Velocity (m/s)
$\mu$	: Dynamic Viscosity (Pa-s)

## Conflict of Interest Statement

The author declares that there is no conflict of interest in the study.

## CRediT Author Statement

**Shalom Akhai:** Investigation, Review, Editing, Data analysis, Conceptualization.

**Amandeep Singh Wadhwa:** Investigation, Editing, Original draft, Conceptualization, Methodology

## References

- [1] He Z, Yan Y, Zhang Z. Thermal management and temperature uniformity enhancement of electronic devices by micro heat sinks: A review. *Energy*. 2021 Feb 1; 216:119223. <https://doi.org/10.1016/j.energy.2020.119223>
- [2] Smoyer JL, Norris PM. Brief historical perspective in thermal management and the shift toward management at the nanoscale. *Heat Transfer Engineering*. 2019 Feb 25; 40(3-4):269-82. <https://doi.org/10.1080/01457632.2018.1426265>
- [3] Niemz MH, Niemz MH. Medical applications of lasers. *Laser-tissue interactions: fundamentals and applications*. 2019:153-249.
- [4] Bhanvase B, Barai D. Nanofluids for Heat and Mass Transfer: Fundamentals, Sustainable Manufacturing and Applications. Academic Press; 2021 Apr 29.
- [5] Viskanta R. Thermal engineering challenges for the 21st century. *energetika*. 2013;59(4).
- [6] Nwaigwe K, Okoronkwo CA, Ogueke NV, Anyanwu EE. Review of nocturnal cooling systems. *International Journal of Energy for a Clean Environment*. 2010;11(1-4). <https://doi.org/10.1615/InterJEnerCleanEnv.2011003225>
- [7] Buzzichelli G, Anelli E. Present status and perspectives of European research in the field of advanced structural steels. *ISIJ international*. 2002 Dec 15;42(12):1354-63. <https://doi.org/10.2355/isijinternational.42.1354>

- [8] National Academies of Sciences, Engineering, and Medicine. The future of atmospheric chemistry research: remembering yesterday, understanding today, anticipating tomorrow. National Academies Press; 2016 Dec 29.
- [9] Zhang Z, Cao B. Thermal smart materials with tunable thermal conductivity: Mechanisms, materials, and applications. Science China Physics, Mechanics & Astronomy. 2022 Nov; 65(11):117003. <https://doi.org/10.1007/s11433-022-1925-2>
- [10] Ukueje WE, Abam FI, Obi A. A perspective review on thermal conductivity of hybrid nanofluids and their application in automobile radiator cooling. Journal of Nanotechnology. 2022 May 30; 2022. <https://doi.org/10.1155/2022/2187932>
- [11] Krishna Y, Faizal M, Saidur R, Ng KC, Aslfattahi N. State-of-the-art heat transfer fluids for parabolic trough collector. International Journal of Heat and Mass Transfer. 2020 May 1;152:119541. <https://doi.org/10.1016/j.ijheatmasstransfer.2020.119541>
- [12] Rubbi F, Habib K, Saidur R, Aslfattahi N, Yahya SM, Das L. Performance optimization of a hybrid PV/T solar system using Soybean oil/MXene nanofluids as A new class of heat transfer fluids. Solar Energy. 2020 Sep 15;208:124-38. <https://doi.org/10.1016/j.solener.2020.07.060>
- [13] Li J, Yang L. Recent Development of Heat Sink and Related Design Methods. Energies. 2023 Oct 18;16(20):7133. <https://doi.org/10.3390/en16207133>
- [14] Wang C, Yu X, Pan X, Qin J, Huang H. Thermodynamic optimization of the indirect precooled engine cycle using the method of cascade utilization of cold sources. Energy. 2022 Jan 1; 238:121769. <https://doi.org/10.1016/j.energy.2021.121769>
- [15] Khan MZ, Younis MY, Akram N, Akbar B, Rajput UA, Bhutta RA, Uddin E, Jamil MA, Márquez FP, Zahid FB. Investigation of heat transfer in wavy and dual wavy micro-channel heat sink using alumina nanoparticles. Case Studies in Thermal Engineering. 2021 Dec 1;28:101515. <https://doi.org/10.1016/j.csite.2021.101515>
- [16] Gao J, Hu Z, Yang Q, Liang X, Wu H. Fluid flow and heat transfer in microchannel heat sinks: Modelling review and recent progress. Thermal Science and Engineering Progress. 2022 Mar 1;29:101203. <https://doi.org/10.1016/j.tsep.2022.101203>
- [17] Driss A, Maalej S, Chouat I, Zaghdoudi MC. Experimental Investigation on the Thermal Performance of a Heat Pipe-based Cooling System. Mathematical Modelling of Engineering Problems. 2019 Jun 1;6(2). <https://doi.org/10.18280/mmep.060209>
- [18] Granado EQ, Pelenghi G, Hijlkema J, Anthoine J, Lestrade JY. A new System Design Tool for a Hybrid Rocket Engine Application. In 73rd International Astronautical Congress (IAC 2022) 2022 Sep 18.
- [19] Tuckerman DB, Pease RF. High-performance heat sinking for VLSI. IEEE Electron device letters. 1981 May;2(5):126-9. <https://doi.org/10.1109/EDL.1981.25367>
- [20] Peng XF, Peterson GP. Forced convection heat transfer of single-phase binary mixtures through micro channels. Experimental Thermal and fluid science. 1996 Jan 1;12(1):98-104. [https://doi.org/10.1016/0894-1777\(95\)00079-8](https://doi.org/10.1016/0894-1777(95)00079-8)
- [21] Kawano K, Minakami K, Iwasaki H, Ishizuka M. Micro channel heat exchanger for cooling electrical equipment. In ASME International Mechanical Engineering Congress and Exposition 1998 Nov 15 (Vol. 26720, pp. 173-180). American Society of Mechanical Engineers. <https://doi.org/10.1115/IMECE1998-0650>
- [22] Yin JM, Bullard CW, Hrnjak PS. Single-phase pressure drop measurements in a microchannel heat exchanger. Heat Transfer Engineering. 2002 Jul 1;23(4):3-12. <https://doi.org/10.1080/01457630290090455>
- [23] Kim SJ. Methods for thermal optimization of microchannel heat sinks. Heat transfer engineering. 2004 Jan 1;25(1):37-49. <https://doi.org/10.1080/01457630490248359>
- [24] Min JY, Jang SP, Kim SJ. Effect of tip clearance on the cooling performance of a microchannel heat sink. International Journal of Heat and Mass Transfer. 2004 Feb 1;47(5):1099-103. <https://doi.org/10.1016/j.ijheatmasstransfer.2003.08.020>
- [25] Xu JL, Gan YH, Zhang DC, Li XH. Microscale heat transfer enhancement using thermal boundary layer redeveloping concept. International Journal of Heat and Mass Transfer. 2005 Apr 1;48(9): 1662-74. <https://doi.org/10.1016/j.ijheatmasstransfer.2004.12.008>
- [26] Lee PS, Garimella SV. Thermally developing flow and heat transfer in rectangular microchannels of different aspect ratios. International journal of heat and mass transfer. 2006 Aug 1;49(17-18):3060-7. <https://doi.org/10.1016/j.ijheatmasstransfer.2006.02.011>
- [27] Wang XD, An B, Xu JL. Optimal geometric structure for nanofluid-cooled microchannel heat sink under various constraint conditions. Energy conversion and management. 2013 Jan 1;65:528-38. <https://doi.org/10.1016/j.enconman.2012.08.018>
- [28] Dixit P, Lin N, Miao J, Wong WK, Choon TK. Silicon nanopillars based 3D stacked microchannel heat sinks concept for enhanced heatdissipation applications in MEMS packaging. Sensors and Actuators A: Physical. 2008 Feb 15;141(2):685-94. <https://doi.org/10.1016/j.sna.2007.09.006>
- [29] Eastman JA, Choi SU, Li S, Yu W, Thompson LJ. Anomalously increased effective thermal conductivities of ethylene glycol-based nanofluids containing copper nanoparticles. Applied physics letters. 2001 Feb 5;78(6):718-20. <https://doi.org/10.1063/1.1341218>
- [30] Chein R, Chen J. Numerical study of the inlet/outlet arrangement effect on microchannel heat sink performance. International Journal of Thermal Sciences. 2009 Aug 1;48(8):1627-38. <https://doi.org/10.1016/j.ijthermalsci.2008.12.019>
- [31] Gunnasegaran P, Mohammed H, Shuaib NH. Pressure drop and friction factor for different shapes of microchannels. In 2009 3rd International Conference on Energy and Environment (ICEE) 2009 Dec 7 (pp. 418-426). IEEE.
- [32] Wang XQ, Mujumdar AS. Heat transfer characteristics of nanofluids: a review. International journal of thermal sciences. 2007 Jan 1; 46(1): 1-9. <http://dx.doi.org/10.1016/j.ijthermalsci.2006.06.010>
- [33] Timofeeva EV, Routbort JL, Singh D. Particle shape effects on thermophysical properties of alumina nanofluids. Journal of applied physics. 2009 Jul 1;106(1). <https://doi.org/10.1063/1.3155999>
- [34] Nguyen CT, Desgranges F, Galanis N, Roy G, Maré T, Boucher S, Mintsa HA. Viscosity data for Al<sub>2</sub>O<sub>3</sub>-water nanofluid—hysteresis: is heat transfer enhancement using nanofluids reliable. International journal of thermal sciences. 2008 Feb 1; 47(2):103-11. <https://doi.org/10.1016/j.ijthermalsci.2007.01.033>
- [35] Duangthongsuk W, Wongwises S. Measurement of temperature-

dependent thermal conductivity and viscosity of TiO<sub>2</sub>-water nanofluids. Experimental thermal and fluid science. 2009 Apr 1; 33(4):706-14.

<https://doi.org/10.1016/j.expthermflusci.2009.01.005>

[36] Putra N, Roetzel W, Das SK. Natural convection of nano-fluids. Heat and mass transfer. 2003 Sep;39(8-9):775-84.

<https://doi.org/10.1007/s00231-002-0382-z>

[37] Ho CJ, Wei LC, Li ZW. An experimental investigation of forced convective cooling performance of a microchannel heat sink with Al<sub>2</sub>O<sub>3</sub>/water nanofluid. Applied Thermal Engineering. 2010 Feb 1; 30(2-3):96-103. <https://doi.org/10.1016/j.applthermaleng.2009.07.003>

[38] Xie H, Lee H, Youn W, Choi M. Nanofluids containing multi-walled carbon nanotubes and their enhanced thermal conductivities. Journal of Applied physics. 2003 Oct 15; 94(8): 4967-71.

<https://doi.org/10.1063/1.1613374>

[39] Akhiani AR, Mehrli M, Tahan Latibari S, Mehrli M, Mahlia TM, Sadeghinezhad E, Metselaar HS. One-step preparation of form-stable phase change material through self-assembly of fatty acid and graphene. The Journal of Physical Chemistry C. 2015 Oct 8; 119 (40):22787-96.

<https://doi.org/10.1021/acs.jpcc.5b06089>

[40] Chon CH, Kihm KD, Lee SP, Choi SU. Empirical correlation finding the role of temperature and particle size for nanofluid (Al<sub>2</sub>O<sub>3</sub>) thermal conductivity enhancement. Applied Physics Letters. 2005 Oct 10; 87(15). <https://doi.org/10.1063/1.2093936>

[41] Ghadimi A, Saidur R, Metselaar HS. A review of nanofluid stability properties and characterization in stationary conditions. International journal of heat and mass transfer. 2011 Aug 1; 54(17-18):4051-68.

<https://doi.org/10.1016/j.ijheatmasstransfer.2011.04.014>